

Salt Thermal Testing in Heated Boreholes: Experiments and Simulations

Fuel Cycle Research & Development

*Prepared for
U.S. Department of Energy
Used Fuel Disposition Campaign
Milestone M3SF-19LA010303011*

*P.H. Stauffer
E.J. Gultinan
S.M. Bourret
G.A. Zyvoloski*

*Los Alamos National Laboratory
March 31, 2019*

Los Alamos National Laboratory Document
LA-UR-19-22729



DISCLAIMER

This information was prepared as an account of work sponsored by an agency of the U.S. Government. Neither the U.S. Government nor any agency thereof, nor any of their employees, makes any warranty, expressed or implied, or assumes any legal liability or responsibility for the accuracy, completeness, or usefulness, of any information, apparatus, product, or process disclosed, or represents that its use would not infringe privately owned rights. References herein to any specific commercial product, process, or service by trade name, trade mark, manufacturer, or otherwise, does not necessarily constitute or imply its endorsement, recommendation, or favoring by the U.S. Government or any agency thereof. The views and opinions of authors expressed herein do not necessarily state or reflect those of the U.S. Government or any agency thereof.

FCT Quality Assurance Program Document

**Appendix E
FCT Document Cover Sheet
Salt Thermal Testing in Heated
Boreholes: Experiments and
Simulations**

Name/Title of Deliverable/Milestone _____
 Work Package Title and Number **SF-19LA010303011** **Salt R&D - LANL**
 Work Package WBS Number **1.08.01.03.03 - Salt Disposal R&D**
 Responsible Work Package Manager **Philip H. Stauffer** *Philip H Stauffer 3/25/19*
 (Name/Signature)

Date Submitted _____

Quality Rigor Level for Deliverable/Milestone	<input checked="" type="checkbox"/> QRL-3	<input type="checkbox"/> QRL-2	<input type="checkbox"/> QRL-1 <input type="checkbox"/> Nuclear Data	<input type="checkbox"/> N/A*
---	---	--------------------------------	---	-------------------------------

This deliverable was prepared in accordance with Los Alamos National Laboratory
 (Participant/National Laboratory Name)

QA program which meets the requirements of
 DOE Order 414.1 NQA-1-2000

This Deliverable was subjected to:

Technical Review

Technical Review (TR)

Review Documentation Provided

- Signed TR Report or,
- Signed TR Concurrence Sheet or,
- Signature of TR Reviewer(s) below

Name and Signature of Reviewers

Hari Viswanathan

[Signature]

Peer Review

Peer Review (PR)

Review Documentation Provided

- Signed PR Report or,
- Signed PR Concurrence Sheet or,
- Signature of PR Reviewer(s) below

*Note: In some cases there may be a milestone where an item is being fabricated, maintenance is being performed on a facility, or a document is being issued through a formal document control process where it specifically calls out a formal review of the document. In these cases, documentation (e.g., inspection report, maintenance request, work planning package documentation or the documented review of the issued document through the document control process) of the completion of the activity along with the Document Cover Sheet is sufficient to demonstrate achieving the milestone. QRL for such milestones may be also be marked N/A in the work package provided the work package clearly specifies the requirement to use the Document Cover Sheet and provide supporting documentation.

Table of Contents

List of Figures V

List of Tables VI

1. Introduction 3

2. Heater Block Experiments and Simulations 5

 2.1 Field Experiments..... 5

 2.2 Heater Block Modeling Development..... 6

 2.3 Model Initialization and Simulation 9

 2.4 Variable Temperature Heater Block Simulations..... 13

 2.5 Radiative Heating Experiments and Simulations 15

 2.6 Summary **Error! Bookmark not defined.**

3. References 21

List of Figures

Figure 1-1: Installation of an infrared heater in the WIPP underground.	4
Figure 2-1: Detailed view of heated borehole instrumentation and B) Layout of heated borehole (HB) and two temperature monitoring boreholes temp hole (TB) and small temp hole (TSB).	5
Figure 2-2: Cross section of the initial heater block mesh.....	6
Figure 2-3: Measured and simulated temperature during a period where the heaters Cross section of the initial heater block mesh	7
Figure 2-4: Cross section of model domains. A) Smaller 3m x 3m x 7m domain. B) Larger 20m x 20m x 10m domain.	8
Figure 2-5: Temperature profile along the axis of the heater.....	9
Figure 2-6: Pressure distribution development for Phase 1 simulation initialization	11
Figure 2-7: Final Simulation of the 120 °C heater block experiment.....	12
Figure 2-8: Water production during the 120 °C heater block experiment.....	13
Figure 2-9: Variable temperature heater block simulation	14
Figure 2-10: Infrared heater being tested on the floor of the mine at WIPP prior to installation	16
Figure 2-11: Simulation of 260W infrared heater experiment.....	17
Figure 3-1: Experimental configuration for Phase 2 experiments. Red contours indicate the temperature simulations from numerical models.	18
Figure 3-2: Pressure field development for the Phase 2 simulations. Unlike the Phase 1 pressure distributions, the simulations do not equilibrate to the freshly drilled boreholes.	19
Figure 3-3: Comparison of the temperatures observed and simulated during the Phase 1 (shakedown) experiments and those predicted by the 750W heater to be used during the Phase 2 experiments.....	20

List of Tables

Table 2-1: Initial salt parameters 10

1

2 **1. Introduction**

3

4 Salt formations may be an ideal repository for heat generating nuclear waste (HGNW)
5 due to their extremely low permeability, high thermal conductivity, self healing capability, and
6 expansive existence in the USA. However, uncertainties associated with brine availability and
7 composition near heat generating waste remains a focus for research (*Bourret et al., 2019,*
8 *Kuhlman et al., 2018*). Heat sources within salt may establish so called “heat pipes” where the
9 boiling of water vapor and subsequent condensing of steam within the formation create a
10 multiphase convection system. While the presence of heated brine may corrode waste canisters
11 the development of “heat pipes” may support storage efforts through the precipitation of salt
12 around the canisters (*Johnson et al., 2019, Jordan et al., 2015, Kuhlman et al., 2013*). To reduce
13 these uncertainties and improve model forecasts for HGNW storage in salt, heated borehole
14 experiments have been proposed at the Waste Isolation Pilot Plant (WIPP) (*Stauffer et al., 2015*).
15 Numerical models are being developed and calibrated at LANL to support the field test design.

16 Work conducted by LANL for Salt R&D during the first half of the 2019 fiscal year
17 includes the development and implementation of the first phase of heated borehole experiments,
18 numerical modeling for generic repository science with potential international applicability, and
19 fundamental code development in support of the heated borehole experiments. This document
20 focuses on the development of numerical models to support the experimental efforts and help
21 design the larger Phase 2 experiments. A brief summary of the experimental progress is included
22 but will be the focus of the annual experimental milestone in August 2019. Model development
23 has been conducted using the porous flow simulator FEHM (Zyvoloski et al. 2012,
24 <https://fehm.lanl.gov>).

LANL 2019 - Experiments and Modeling to Support Field Test Design

25 Phase 1 of the heated borehole experiments was conducted as a “shakedown”. Its
26 purpose was to learn the logistical challenges of working underground at WIPP while working
27 through technical challenges in the field test design before the larger, and more expensive, Phase
28 2 experiment. The Phase 1 experiments began in July, 2018 and continued throughout the first
29 half of the 2019 fiscal year. The most important aspects of the Phase 1 experiments for model
30 development have been the implementation of three different heat sources and the monitoring of
31 water production during the tests. Results from the Phase 1 experiments allowed LANL to
32 develop and calibrate numerical models that were used to inform the design of the larger Phase 2
33 experiments. A detailed summary of Phase 1 of the heated borehole experiments can be found in
34 *Kuhlman et al.* [2018]. Work has begun on the implementation of Phase 2, which will be
35 detailed in a future milestone report.



36
37

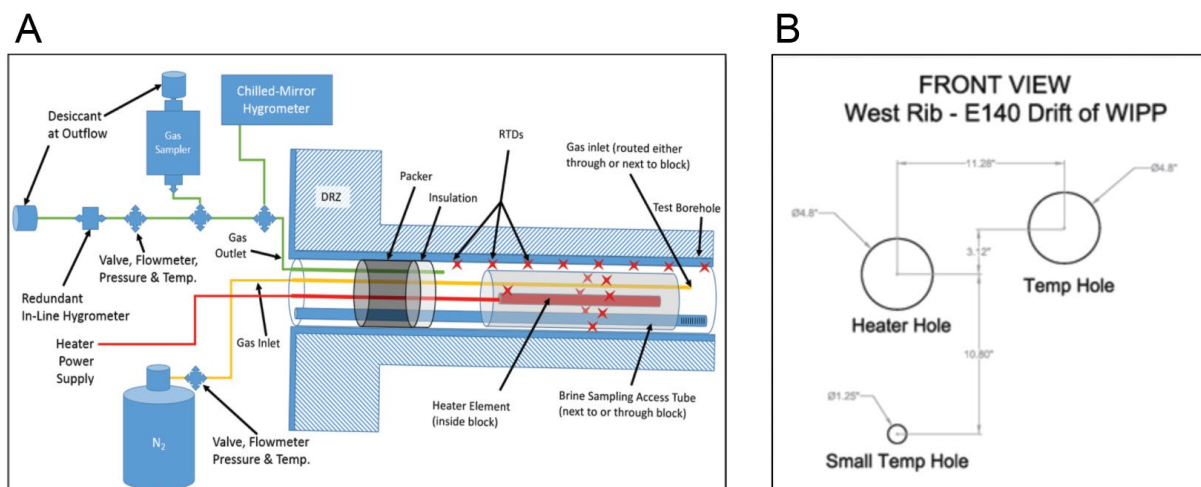
Figure 1-1: Installation of an infrared heater in the WIPP underground.

38 2. Phase 1: “Shakedown” Experiments and Simulations

39 2.1 Field Experiments

40

41 During the Phase 1 experiments boreholes previously drilled in the WIPP underground
 42 were used to test different experimental setups. The initial test design relied upon the use of a
 43 stainless steel heater block which could be set to prescribed temperatures (Figure 2-1A). Besides
 44 the heated borehole (HB) temperature sensors were also deployed in two adjacent boreholes
 45 (Temp Hole – TB; and Small Temp Hole -TSB) to monitor the temperature distribution within
 46 the salt (Figure 2-1B).



47

48 *Figure 2-1: Detailed view of heated borehole instrumentation and B) Layout of heated borehole (HB) and two temperature*
 49 *monitoring boreholes temp hole (TB) and small temp hole (TSB).*

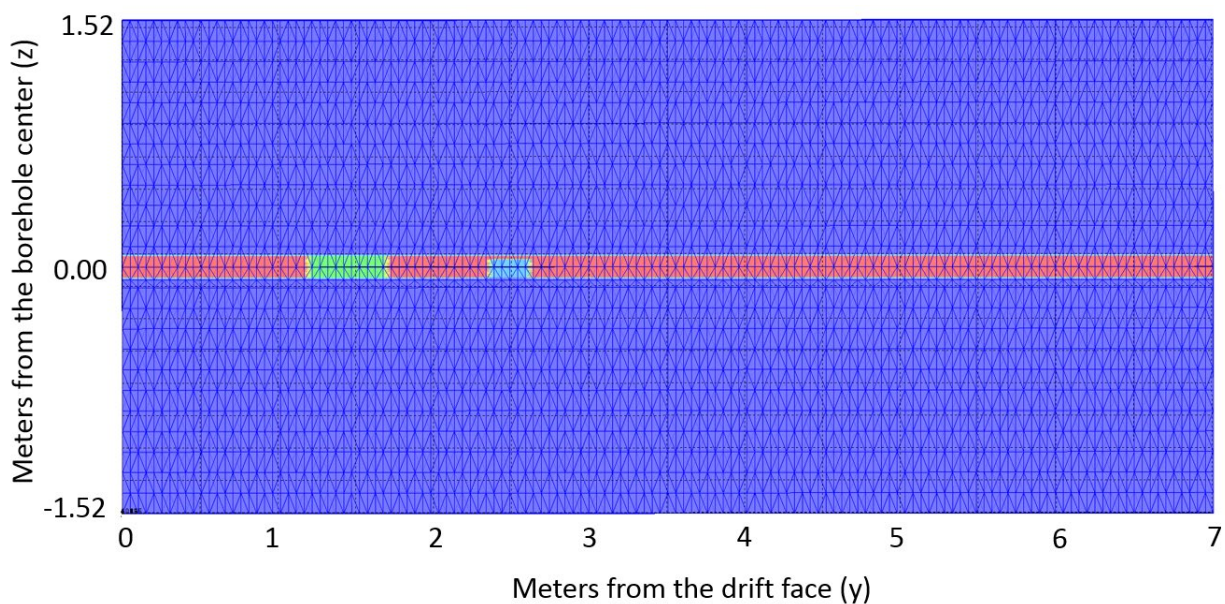
50

51 With a goal of producing a temperature rise of 120° C within the salt, the heater block
 52 was set to 120° C. However, the air gap around the heater block insulated the formation from the
 53 heater creating a poor thermal coupling between the salt and heater. This resulted in observed
 54 temperatures within the temperature boreholes of only 35 °C, a 3.5°C degree increase from the
 55 background formation temperature. Although, the temperature rise was less than predicted these
 56 experiments provided valuable data for calibrating and developing numerical models.

57 2.2 Heater Block Modeling Development

58

59 To simulate the heater block experiments a three dimension mesh was generated that is
 60 approximately 3m x 3m x 7m (Figure 2-2) with the center of borehole laying at $x=0, z=0$. The
 61 mesh is highly refined near the borehole and the resolution decreases radially. This results in a
 62 mesh that includes 238,107 elements.



63

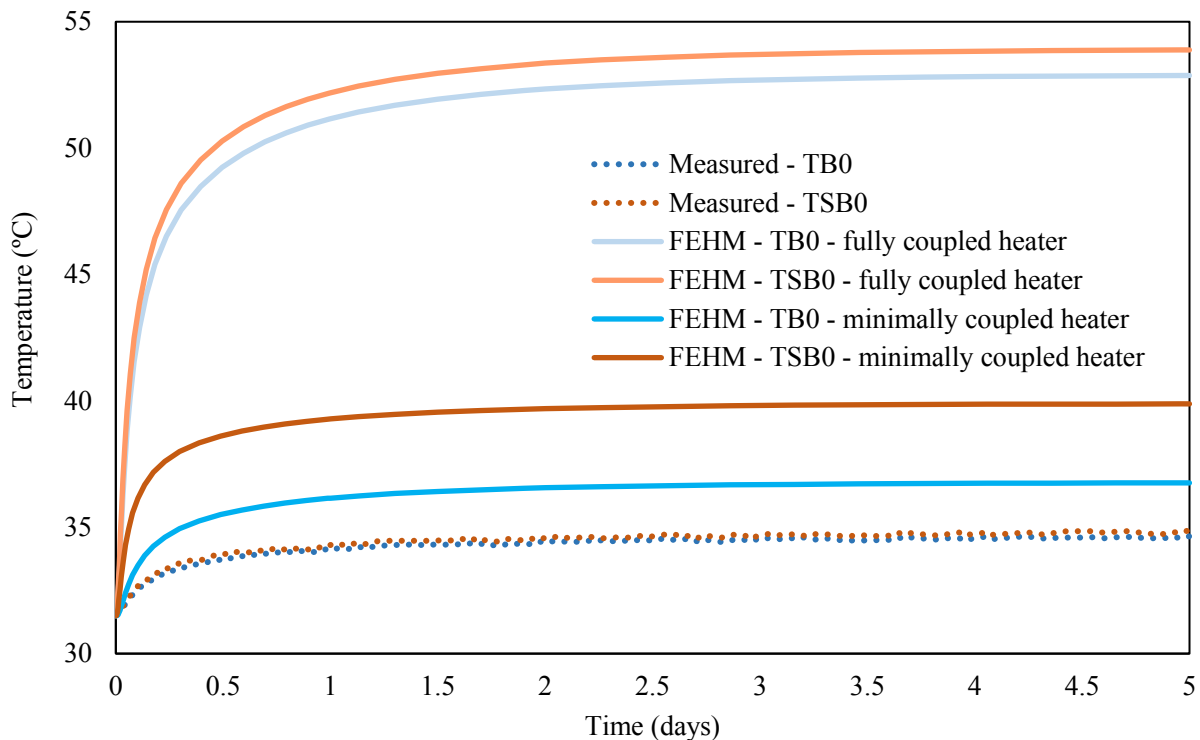
64

Figure 2-2: Cross section of the initial heater block mesh

65

66 Thermal properties of the formation salt can be determined through experimentation and
 67 modeling of time-dependent heat response to the heater in adjacent boreholes (TB and TSB
 68 shown in Fig. 2-1b). Initial simulations of the Phase 1 experiment assumed full coupling between
 69 the heater and the borehole wall in the HB. However, these preliminary simulations over
 70 predicted the transfer of heat into the formation. This result can be seen in Figure 2-3, which
 71 shows the measured temperature in TB and TSB compared to simulated results. The featured

72 thermistors TB0 and TSB0 are located on the same depth from the drift wall as the heater in the
 73 TB and TSB holes, respectively.



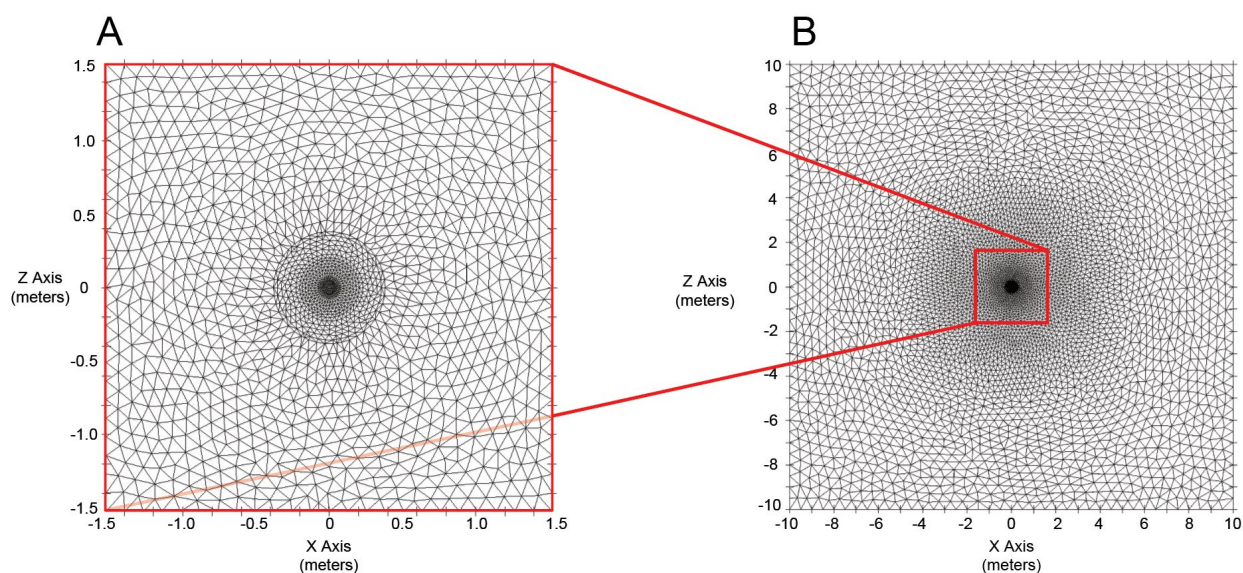
74

75 *Figure 2-3: Measured and simulated temperature during a period where the heaters Cross section of the initial heater block*
 76 *mesh*

77

78 To address the discrepancy between the simulated and measured temperature results, the
 79 simulations were modified to add an air gap around the heater in the HB. While the fully-coupled
 80 simulation assumed full contact between the wall and heater, the minimally-coupled heater
 81 simulations assume only direct contact to the salt on the bottom of the HB where the heater rests.
 82 This allows for thermal insulation around the heater due to the low thermal conductivity of air in
 83 the HB. Fig. 2-3 includes the minimally-coupled simulation, and while this case still over
 84 predicts the temperature at TB0 and TSB0, the simulated transfer of heat is much more
 85 satisfactorily reproduced if an air gap is assumed to be present.

86 To further improve the accuracy of the simulations a larger domain was developed. The
 87 original domain is highly refined around the borehole, but was limited in size due to
 88 computational expense (Figure 2-4a). However, the implementation of a larger, 20m x 20m x
 89 10m model domain (Figure 2-4b) revealed that the boundary conditions in the smaller model
 90 were causing a feedback between the coupled temperature and thermal conductivity producing
 91 an over estimation of the temperature near the borehole.



92
 93 *Figure 2-4: Cross section of model domains. A) Smaller 3m x 3m x 7m domain. B) Larger 20m x 20m x 10m domain.*

94
 95 To accurately model the complex thermo-hydro-mechanical-chemical processes
 96 associated with the heater tests many coupled processes must be included in the model. These
 97 coupled processes can sometimes result in non-intuitive model behavior which leads to a better
 98 understanding of the system. By moving the 31.5 °C temperature boundary condition due to the
 99 background formation temperature further away from the borehole a more accurate temperature
 100 profile is produced (Figure 2-5).

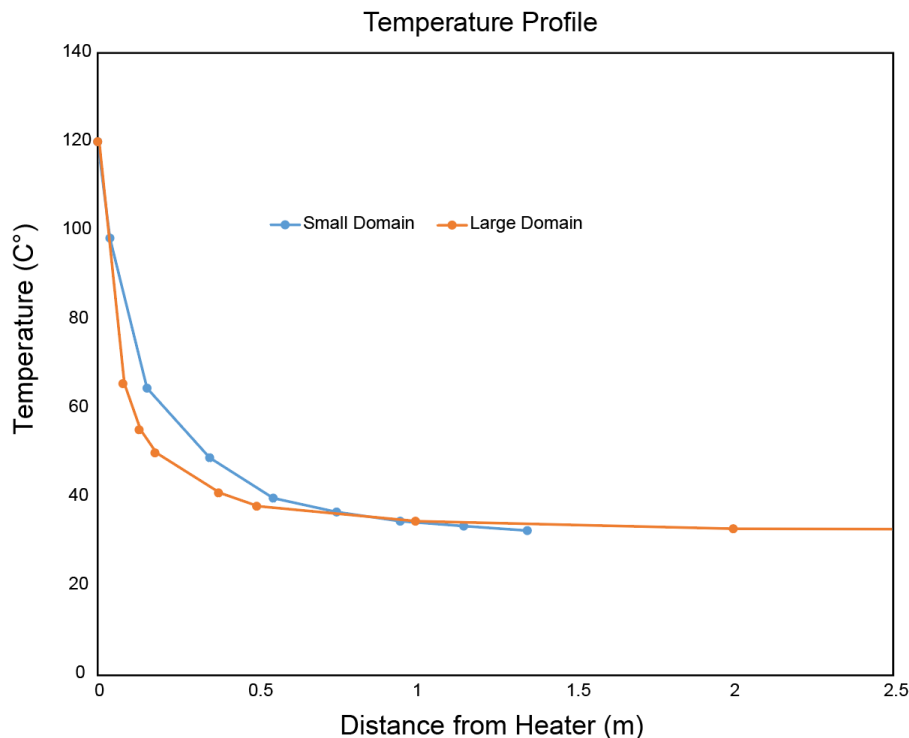


Figure 2-5: Temperature profile along the axis of the heater.

101

102

103

104

105 2.3 Model Initialization and Simulation of Heater Block

106

107 Beginning with accurate initial conditions is critical to model accuracy. Table 3-1
 108 displays the initial properties of the intact salt used during the simulations. These properties are
 109 dependent upon each other and vary throughout model. For instance, porosity changes due to the
 110 dissolution of salt drive changes in permeability; whereas, temperature changes from the heater
 111 drive changes in thermal conductivity. The implementation of these coupled processes in FEHM
 112 have been developed over the years with some recent work on the variable thermal conductivity
 113 and permeability of salt being covered in the previous modeling milestone (*Johnson et al., 2018*)

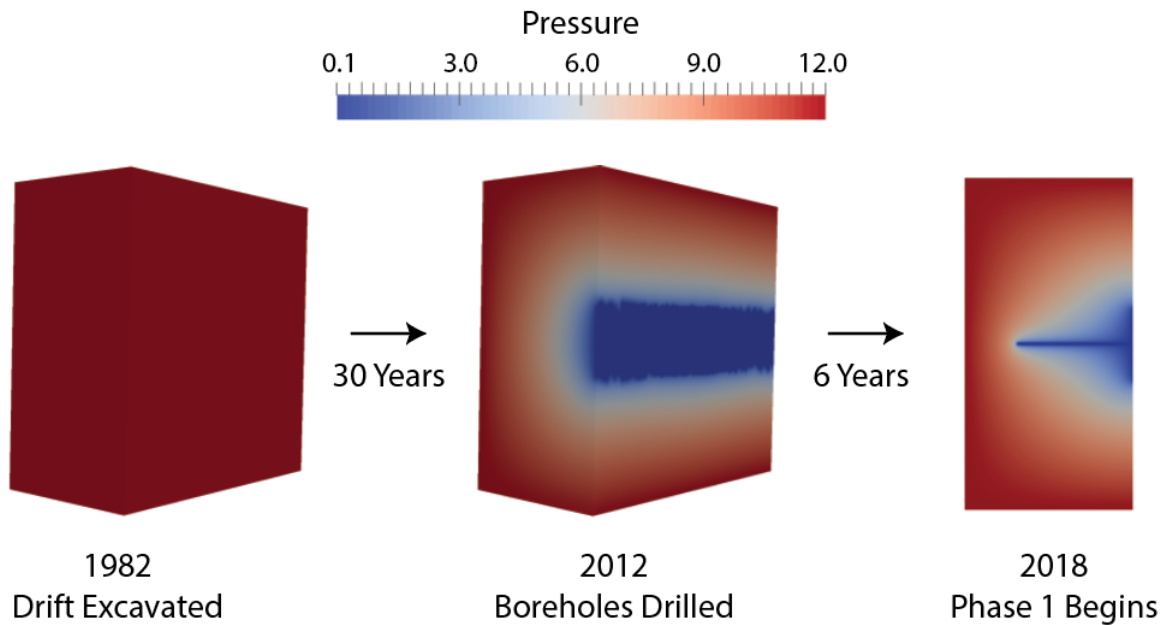
114

115 *Table 2-1: Important Initial parameters used for Phase 1 salt simulations*

Parameter	Value
Salt initial porosity (-)	0.001
Salt initial permeability (m ²)	10 ⁻²¹
Salt initial thermal conductivity (W/m K)	5.25
Initial formation pressure (MPa)	12
Initial formation temperature (°C)	31.5
Residual saturation (-)	0.1

116

117 Due to the extremely low permeability of intact salt, field measurements of formation
118 pressure are difficult. Previous work indicates that in the undisturbed salt near WIPP the
119 formation pressure is approximately 12 MPa (Beauheim 1999). Using this information and
120 knowledge of the mining activities at WIPP we developed an estimated pressure distribution at
121 the location of the heated borehole in the E140 drift. First, the model is initialized at 12 MPa
122 throughout the domain, this represents the formation prior to the excavation of the mine (Figure
123 2-6). Next an atmospheric boundary condition is applied along one side, this represents the
124 initial mining of the E-140 drift in 1982, and the model is allowed to equilibrate for 30 years.
125 After 30 years of model time, the domain is further updated to include the heated borehole, this
126 corresponds to the drilling of these boreholes in 2012. Next the model is run for an additional 6
127 years to arrive at the pressure conditions within the formation at the start of the Phase 1 testing.
128 This final condition is then used as the initial pressure distribution condition for each of the
129 Phase 1 simulations.



130

131

Figure 2-6: Pressure distribution development for Phase 1 simulation initialization

132

133

134

135

136

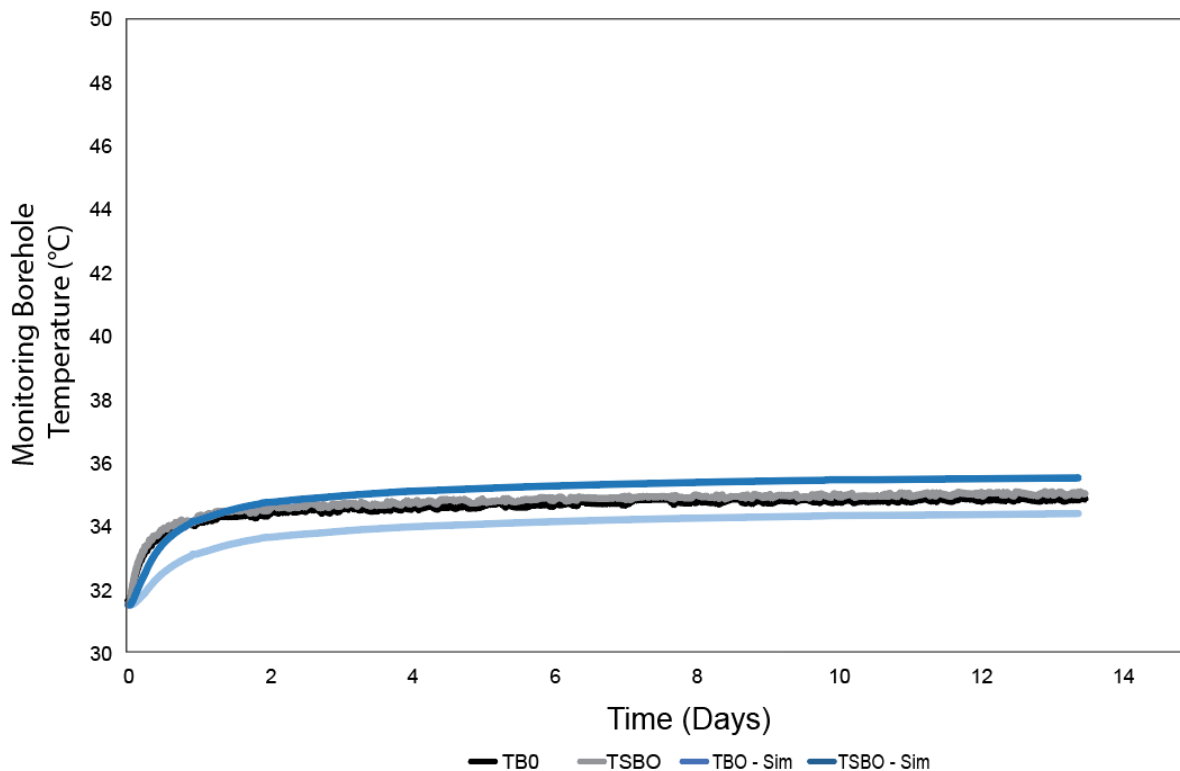
137

The final constant 120 °C Phase 1 heater simulation temperature results are shown in Figure 2-7. The model is able to accurately represent the temperature at the monitoring locations to within 2 degrees. Some error associated with measuring the precise locations of the temperature sensors within boreholes that are not entirely straight is considered a likely reason for this discrepancy.

138

139

140



141

142

Figure 2-7: Final Simulation of the 120 °C heater block experiment

143 During this experiment water vapor was extracted from behind the packer by circulating nitrogen

144 throughout the test. We find that a permeability of $1e-21$ m² produces a fairly accurate

145 simulation of the water production (Figure 2-8), but the match would likely be better with a

146 slightly lower permeability. Permeability in the damaged zone around the boreholes is likely

147 significantly higher than $1e-21$, but because these boreholes were drilled 6 years prior to the

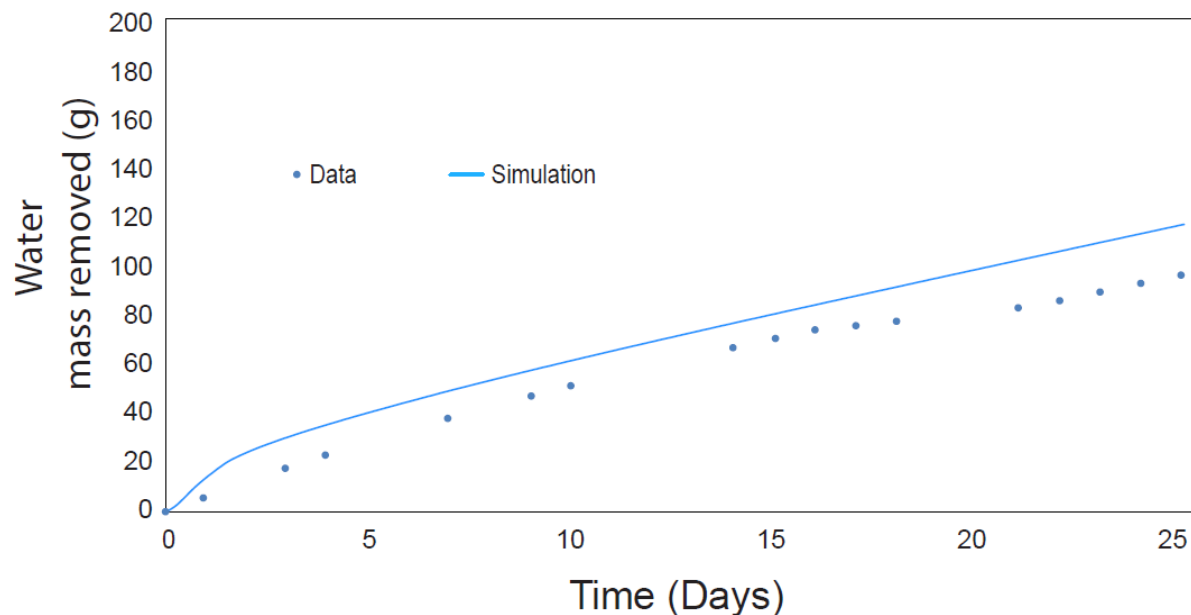
148 Phase 1 testing they have equilibrated and the water flow is now likely controlled by the

149 permeability of the intact salt. The much smaller than expected temperature change means the

150 thermal expansion of the water in the formation had little effect on the flow. The Phase 2 testing,

151 which will use freshly drilled boreholes and significantly more heat will explore brine

152 availability during these tests.



153

154

Figure 2-8: Water production during the 120 °C heater block experiment

155

156 2.4 Variable Temperature Heater Block Simulations

157

158

In an attempt to reach the target formation temperature of 120 °C the heater block

159

temperature was raised in stepwise fashion while monitoring the temperature in the monitoring

160

boreholes. The heater block was subsequently set at 120, 155, 185, and 222 °C over the course

161

of 10 days (Figure 2-9).

162

163

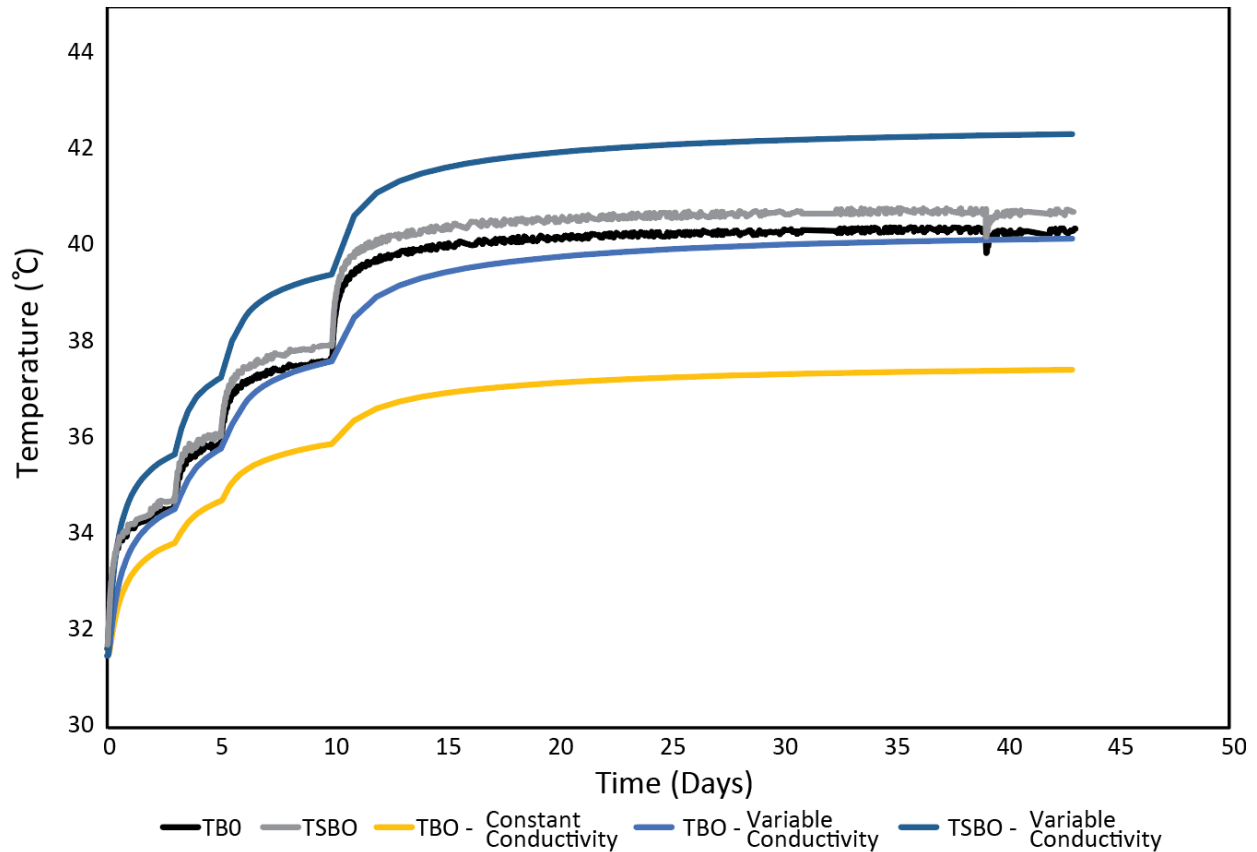


Figure 2-9: Variable temperature heater block simulation

164
165
166

167 Using the same constant thermal conductivity for the insulating air around the heater block we
 168 found the simulations to underestimate the borehole temperatures by a few degrees (yellow line,
 169 Figure 2-9). In order to accurately produce the higher temperatures associated with this
 170 experiment a new variable conductivity algorithm was added to the FEHM source code. This
 171 update to vcon.f, allows for the energy from black body radiation between two nodes to be
 172 accounted for through an adjustment of the thermal conductivity. The energy flux due to black
 173 body radiation is proportional to the difference in the temperature to the fourth power (Eq. 1)

174

$$q_{rad} = A_1 F_{1-2} \sigma (T_1^4 - T_2^4) \quad \text{Eq. 1}$$

175

176 where A_1 is the surface area of the heater, T_1 is the temperature of the heater, T_2 is the
 177 temperature of the salt adjacent to the borehole, F_{1-2} is a shape factor, and σ is the emissivity of
 178 the stainless steel heater. In this case, since all of the radiation from the heater impacts the salt
 179 our shape factor is 1. Using this energy flux we can determine the change in thermal
 180 conductivity necessary to account for this radiation, K_R as:

181

$$182 \quad K_R = \frac{q_{rad}H}{A_1(T_1 - T_2)} \quad \text{Eq. 2}$$

183 where H is the size of the air gap in the borehole. Finally, the effective thermal conductivity is
 184 simply the sum of the thermal properties of the air and those due to radiation:

$$185 \quad K_{eff} = K_R + K_{Air} \quad \text{Eq. 3}$$

186 Applying this variable thermal conductivity model we achieve a satisfactory match to the
 187 experimental data (Figure 2-9). Some error is likely be due to the location of the temperature
 188 sensors as well as the selection of an appropriate emissivity factor which varies by material,
 189 temperature, and over time. Unfortunately, even with the heater set to 222 °C, we still only
 190 achieve about 40 °C at the temperature boreholes.

191 **2.5 Radiative Heating Experiments and Simulations**

192

193 In an attempt to increase the thermal coupling between the heater and the formation a 22
 194 inch long quartz infrared heater was selected (Figure 2-10).



195
196 *Figure 2-10: Infrared heater being tested on the floor of the mine at WIPP prior to installation*
197

198 This heater overcomes the insulating layer of air by emitting infrared radiation directly
199 into the formation. The first experiment utilized a 260W heater which achieved 44 °C at the
200 temperature boreholes. This type of heater is accurately modeled using an energy flux boundary
201 condition in FEHM (Figure 2-11).

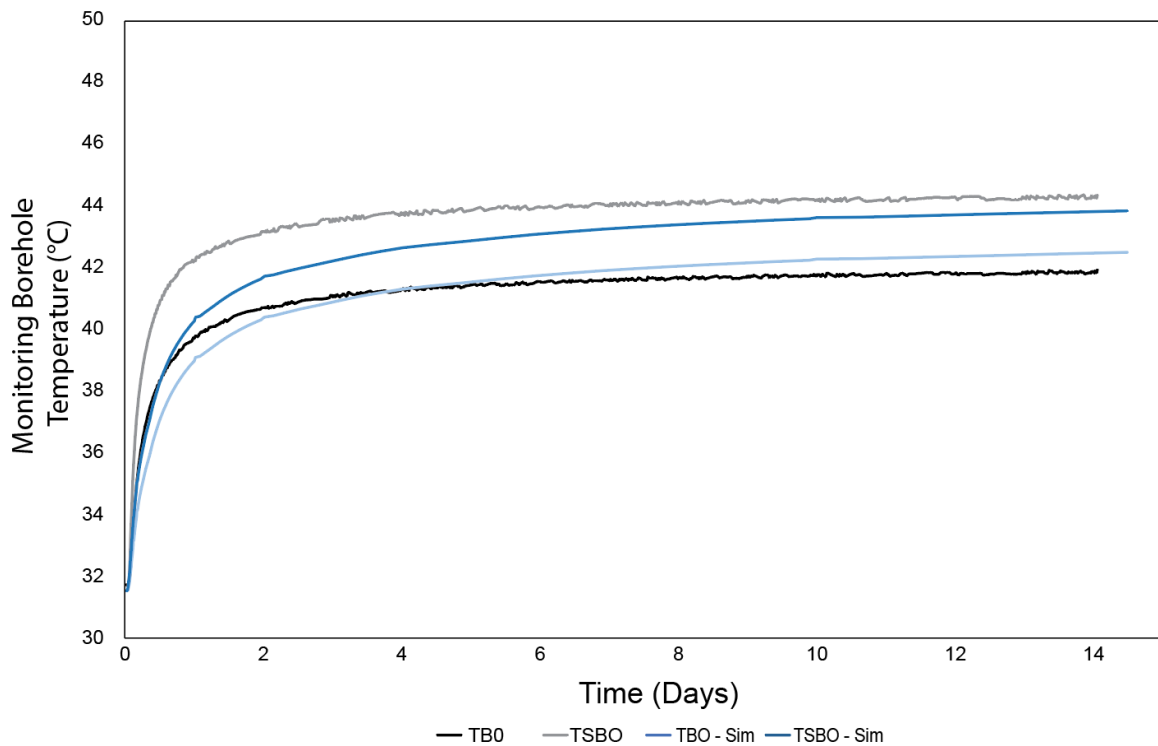


Figure 2-11: Simulation of 260W infrared heater experiment

202

203

204

205

206

207

208

209

210

211

212

213

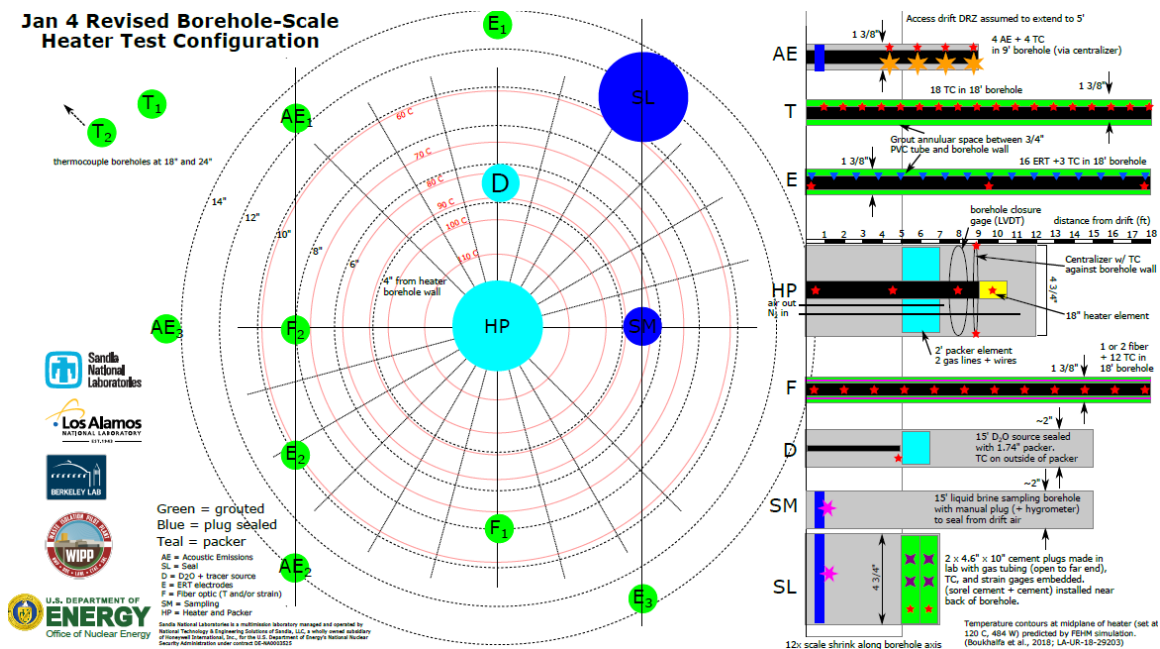
Successful simulations of the 260W heater experiment provided confidence in the model allowing for the selection of a heater with a specific wattage to achieve the targeted temperature goals. Simulations showed that 750W would achieve approximately 140 °C at the borehole wall and ** at the temperature boreholes. At the time of this writing the 750W has achieved 144 °C at the borehole wall and data from the temperature boreholes is not yet available. With this heater achieving the desired temperatures the Phase 1 experiments are complete. The boreholes for Phase 2 are currently being drilled and the modeling and experiments from them will be the subject of future milestones.

214 **3. Phase 2 Experiments and Simulations**

215

216 The borehole pattern for the Phase 2 experiments is currently being drilled in the WIPP
 217 underground. The Phase 2 experiments will include electrical resistivity measurements, acoustic
 218 emission monitoring, more temperature monitoring locations, and tracer injection and sampling
 219 locations (Figure 3-1).

220



221

222 *Figure 3-1: Experimental configuration for Phase 2 experiments. Red contours indicate the temperature simulations from*
 223 *numerical models.*

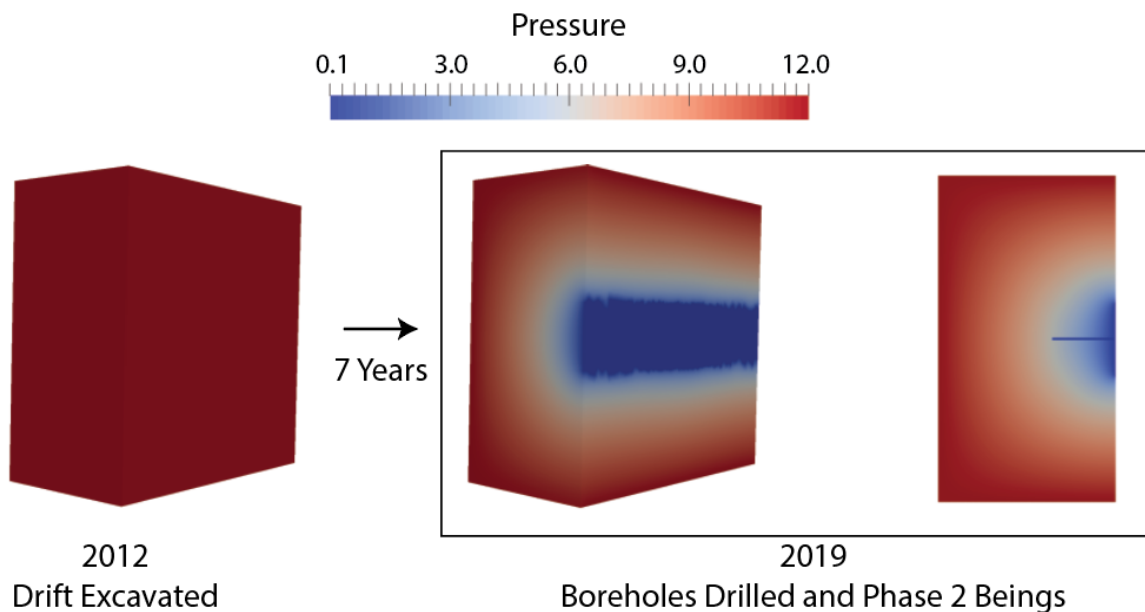
224

225 The red contours on Figure 3-1 indicate the temperature contours from the numerical simulations
 226 developed during the first half of fiscal 2019 at LANL. These simulations have been critical to the
 227 selection of a 750W infrared heater and the final borehole configuration for the Phase 2 experiments.

228 The drift where the Phase 2 experiments are being installed was excavated in early 2012. The
 229 pressure distribution was developed similarly to the Phase 1 simulations; however, because the

LANL 2019 - Experiments and Modeling to Support Field Test Design

230 boreholes are being freshly drilled the pressure distribution is not allowed to equilibrate around the
 231 boreholes (Figure 3-2). Characterizing the water availability in freshly disturbed boreholes is an
 232 important aspect of the Phase 2 experiments and simulations.

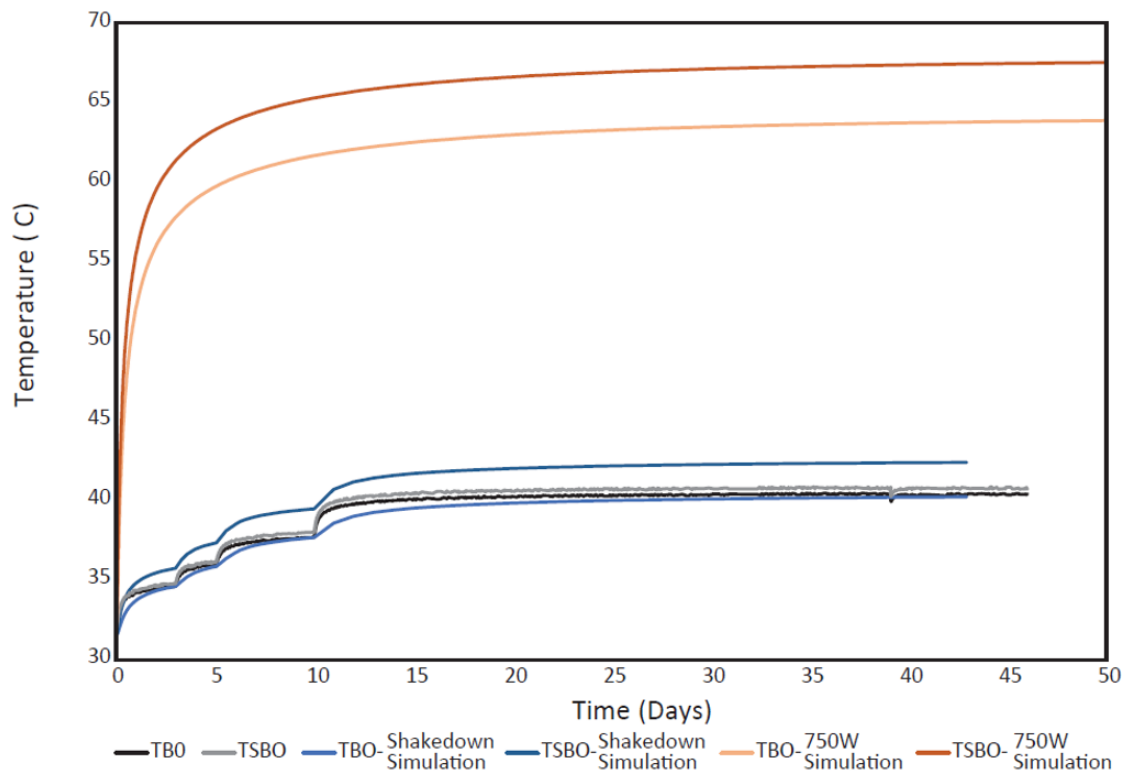


233
 234 *Figure 3-2: Pressure field development for the Phase 2 simulations. Unlike the Phase 1 pressure distributions, the simulations*
 235 *do not equilibrate to the freshly drilled boreholes.*

236

237 The 750W heater selected for the Phase 2 experiments is expected to raise the temperature
 238 significantly more than the Phase 1 experiments. The simulations predict the area around the borehole
 239 to approach 140 °C with the temperatures reaching approximately 65 °C as far out as the Phase 1
 240 temperature boreholes (Figure 3-3). As far as 1 meter away from the heated borehole temperatures are
 241 forecast to still be above 40 °C. This significant increase in temperature will allow for the study of the
 242 thermal effects on water availability that were not observable during the Phase 1 experiments.

243



244

245 *Figure 3-3: Comparison of the temperatures observed and simulated during the Phase 1 (shakedown) experiments and those*
 246 *predicted by the 750W heater to be used during the Phase 2 experiments*

247

248 The Phase 1 experiments have provided an excellent opportunity for model development and
 249 calibration and provided confidence in the successful implementation of the Phase 2 experiments and
 250 modeling. The FEHM simulations accurately represent the temperature of the salt formation and the
 251 simulated pressure distributions and permeability are able to recreate the observed water production.
 252 The Phase 2 experiments will begin shortly and the results of the experiments and simulations will be
 253 the focus of the next modeling milestone.

254

255

256 4. References

257

- 258 Beauheim, R. L., P. S. Domski, and R. M. Roberts (1999), *Hydraulic Testing of Salado*
259 *Formation Evaporites at the Waste Isolation Pilot Plant Site: Final Report*, Sandia
260 National Laboratory, Report: SAND--98-2537
261
- 262 Bourret, S. M., E. J. Guiltinan, P. J. Johnson, S. Otto, D. J. Weaver, B. Dozier, H. Boukhalfa, T.
263 A. Miller, and P. H. Stauffer (2019), *Experiments and Simulation of a Borehole in Salt to*
264 *Understand Heat, Brine, and Vapor Migration*. Waste Management 2019 Proceedings
- 265 FEHM (2019), FEHM Website, <https://fehm.lanl.gov/> accessed March 20th, 2019.
- 266 Johnson, P. J., P. H. Stauffer, G. A. Zyvoloski, and S. M. Bourret (2018), *Experiments and*
267 *Modeling to Support Field Test Design*, Los Alamos National Laboratory, Report: LA-
268 UR-18-28189
269
- 270 Johnson, P. J., S. Otto, D. J. Weaver, B. Dozier, T. A. Miller, A. B. Jordan, N. G. Hayes-Rich,
271 and P. H. Stauffer (2019), *Heat-Generating Nuclear Waste in Salt: Field Testing and*
272 *Simulation*, Vadose Zone Journal, 18(1), doi: 10.2136/vzj2018.08.0160
273
- 274 Jordan, A.B., Boukhalfa, H., Caporuscio, F.A., Stauffer, P.H. *Brine Transport Experiments in*
275 *Granular Salt* (2015), Los Alamos National Laboratory, Report: LA-UR-15-26804.
- 276 Kuhlman, K. L., M. M. Mills, and E. N. Matteo (2017), *Consensus on Intermediate Scale Salt*
277 *Field Test Design*, Sandia National Laboratory, Report: SAND2017-3179R
278
- 279 Kuhlman, K. L., M. M. Mills, C. G. Herrick, E. N. Matteo, P. Stauffer, P. Johnson, H.
280 Boukhalfa, D. Weaver, J. Rutqvist, and Y. Wu (2018), *Project Plan: Salt in Situ Heater*
281 *Test*, Sandia National Laboratory, Report: SAND-2018-4673R
- 282 Kuhlman, K.L., Malama, B (2013), *Brine Flow in Heated Geologic Salt*, Sandia National
283 Laboratory, Report: SAND2013-1944
- 284 Stauffer, P.H., A. B. Jordan, D. J. Weaver, F. A. Caporuscio, J. A. Ten Cate, H. Boukhalfa, B. A.
285 Robinson, D. C. Sassani, K. L. Kuhlman, E. L. Hardin, S. D. Sevougian, R. J.
286 MacKinnon, Y. Wu, T. A. Daley, B. M. Freifeld, P. J. Cook, J. Rutqvist, and J. T.
287 Birkholzer, (2015). *Test proposal document for phased field thermal testing in salt*. Los
288 Alamos National Laboratory, Report: FCRD-UFD-2015-000077
- 289 Zyvoloski, G.A., B. A. Robinson, Z. V. Dash, S. Kelkar, H. S. Viswanathan, R. J. Pawar, P. H.
290 Stauffer, T. A. Miller, S. P. Chu (2012), *Software users manual (UM) for the FEHM*
291 *Application Version 3.1-3.X*, Los Alamos National Laboratory, Report: LA-UR-12-
292 24493

293

294